



Racing bicycle tyres: experimental indoor evaluation of relaxation length

G. Dell'Orto · F. M. Ballo · G. Mastinu · M. Gobbi · G. Magnani

Received: 5 January 2023 / Accepted: 20 June 2023
© The Author(s) 2023

Abstract The paper presents the measurement of the relaxation length of road racing bicycle tyres. In the paper the relaxation length is given as the ratio between cornering stiffness and lateral stiffness of the tyre. Tests were performed with *VeTyT*, a test-rig specifically designed for measuring the lateral characteristics of bicycle tyres. The results from road racing bicycle tyres of two different brands are discussed. Then, a comparison is presented between of 26 mm and 28 mm wide racing tyres. The tyres were tested both on a flat track and on a drum of 2.6 m diameter. The relaxation length for tests on flat track resulted to be on average 15% higher than the ones on drum, for the same vertical load and inflation pressure. In addition, the large role played by inflation pressure on the relaxation length was discovered. Since the relaxation length may affect the bicycle dynamics, the study provides the first quantitative information for the further development of safer and more performant bicycles.

Keywords Lateral characteristics · Inflation pressure · Test-rig · Dynamics · Wobble

G. Dell'Orto (✉) · F. M. Ballo · G. Mastinu · M. Gobbi
Department of Mechanical Engineering, Politecnico di Milano, Via La Masa 1, 20156 Milan, Italy
e-mail: gabriele.dellorto@polimi.it

G. Magnani
Department of Electronics, Information and Bioengineering (DEIB), Politecnico di Milano, Via Ponzio 34/5, 20133 Milan, Italy

1 Introduction

In this paper, the relaxation length has been evaluated for bicycle tyres, by varying vertical load, inflation pressure and rolling surface. The relaxation length related to the lateral force has been exclusively considered since it has the largest effect on the stability of the bicycle [1].

Bicycle dynamics has been studied since the last decade of nineteenth century [2, 3]. Bicycles are featured by large camber angles when moving along a curvilinear path [4, 5], so that tyre properties are very important for stability and handling. Tyre is the only part of the vehicle conceived to connect the vehicle itself to the ground. The interaction between tyre and ground is therefore crucial for vehicle dynamics [6, 7]. This aspect is even more important for single-track vehicles, for which tyre properties may largely affect the stability and safety [8, 9]. Realistic dynamic simulations need therefore to be updated with accurate tyre parameters [10].

With reasonable approximation, the lateral tyre dynamics can be described by a first order differential equation, where the time constant is given by the relaxation length divided by the speed [11]. The relaxation length is a transient property parameter of tyres which describes the lag of the tyre response when subjected to a sudden variation of slip angle [12].

Despite the large role played by tyres on bicycle dynamics [13], very few studies have been published on this topic. Most of them are focused on car

or motorcycle tyres [9]. The role of the tyre relaxation length on the stability of motorcycles has been addressed in [14, 15]. A proper representation of motorcycle dynamic characteristics needs the introduction of tyre relaxation properties [14]. In particular, weave and wobble modes can be considerably affected by variations of tyre parameters. Increasing the value of relaxation length leads to the destabilization of a single-track vehicle. In [16], the stability of a new motorcycle with four wheels is studied considering linear differential equations for tyres. In [17] an advanced multi-body code for motorcycle modeling takes into account the tyre transient response (i.e. relaxation length).

The relaxation length was estimated for motorcycle and scooter tyres in [18], for inflation pressure ranging from 0.5 to 4 bar. Considering the rigid ring model [19], a modal analysis of the tyre was presented, and the stiffness properties were identified. The results were then compared with those derived from experimental tests performed on test-rig at University of Padua [20, 21], with a difference of 20% for radial tyres inflated at 2 bar. Considering diagonal tyres, the difference was found to be 30–50%, showing the necessity of experimental tests.

Based on the results related to motorcycles, similar behavior is expected for bicycles. The occurrence of dynamic instabilities like wobble [22, 23] may be affected by tyre parameters [24]. Specifically, relaxation length and cornering stiffness were found to be among the most influential parameters for wobble [25]. Similar conclusions were also drawn in [26]. Cornering stiffness and relaxation length are strictly related to tyre inflation pressure and, according to the simulations on a Whipple model extended by lateral slipping [3], they might cause the destabilization of wobble mode.

A study on the influence of tyre forces on bicycle stability was also addressed in [27]. The relaxation length was discovered to affect the occurrence of wobble mode. In particular, an increase in relaxation length together with a decrease in cornering stiffness destabilized the wobble mode. Furthermore, the introduction of relaxation length into the tyre model added new high frequencies unstable modes.

A set of simulations was performed in [28] to analyze the influence of geometrical, compliance and tyre parameters on road racing bicycle stability. Using a hands-on bicycle model presented in [24],

it was discovered that the stability of wobble model decreased with an increase in relaxation length.

The relaxation length for light scooter tyres was identified in [18], using proper test-rig [8, 29]. They applied harmonic excitations and measured the input motion with a gyro. Lateral force was recorded by load cell of the test-rig. Signals were then fitted with sine functions, and the phase lag was calculated to derive the relaxation length. In [30], cornering stiffness and lateral stiffness were evaluated for bicycle tyres.. Then, the relaxation length was evaluated as the ratio between cornering stiffness and lateral stiffness, as suggested in [9].

Despite the important role played by tyre parameters in bicycle dynamics, only a few studies on the measurement of tyre characteristics can be found in literature [20]. This is mainly due to the difficulties in performing measurements with a low signal-to-noise ratio [20]. The evaluation of relaxation length is even more rarely addressed by researchers, and a set of accepted parameters for each kind of tyre is still not available.

This paper aims to provide an accurate measurement of the relaxation length for racing bicycle tyres, trying to close the gap on the lack of data in this field of research. In this way, we are contributing to build a database to enable parametric analysis of different bicycles, continuing the work of Moore et al. [10].

The measurement of tyre characteristics presented in this paper are performed through *VeTyT (Velo Tyre Testing)* [31, 32], a test-rig specifically designed for measuring the mechanical characteristics of bicycle tyres, located at the Department of Mechanical Engineering of Politecnico di Milano. Tests were performed on 26 mm and 28 mm wide road racing bicycle tyres from two different market leader brands. In addition, a comparison between results on flat track and on Ruota-Via, a 2.6 m diameter drum [33], was performed.

The measurement of the relaxation length was made in this paper resorting to the lumped parameter model by Von Schlippe-Dietrich [9, 34]. In such a model the tyre contact is a point, and the lateral compliance is given by a simple spring. In this case the relaxation length is simply the ratio between the cornering stiffness and the lateral stiffness. For sake of simplicity, we do not perform the measurement in the time domain of the rising lateral force due to a slip step. This limits our investigation to constant tyre forces and small lateral slips, the latter condition being generally the case for road racing bicycle tyres.

The paper is structured as follows. An introduction to the theory related to relaxation length is given in paragraph 1.1. After that, the methods and instruments used for this study are presented in Sect. 2. The test-rig *VeTyT* exploited for measurements is presented as well as the implemented set-up and the fitting methods for modeling experimental data. In Sect. 3, the results of measurements of lateral stiffness and cornering stiffness are summarized. Finally, Sect. 4 collects the results of relaxation length and the discussion.

1.1 Relaxation length

The relaxation length is an important parameter that characterizes the dynamic response of pneumatic tyres. It affects bicycle handling and its stability. It is defined as the distance a tyre covers before reaching 63% of the steady state value of the lateral force, after a step variation in the slip angle [12].

In case the vertical force F_z is constant, the transient lateral force generated by a tyre can be estimated by resorting to a simple lumped parameter model [9, 12, 34]. The model is described by the following first order differential Eq. (1)

$$\frac{\lambda}{v} \frac{dF_y}{dt} + F_y = \bar{F} \tag{1}$$

where F_y [N] is the lateral force, \bar{F} [N] is the steady state value of lateral force, λ [m] is the relaxation length, v [m/s] is the forward velocity and $\frac{\lambda}{v}$ [s] (also defined τ) is the time constant. Equation (1) can be solved by obtaining (2)

$$F_y = \bar{F} \left(1 - e^{-\frac{\lambda}{v}t} \right) \tag{2}$$

The solution can be plotted, as in Fig. 1. The lines with different colors refer to different tyres. The tyre presented by red line performs better than the others, since at the same speed the time constant τ is smaller, so that tyre reaches faster the steady state conditions.

The relaxation length can be directly measured by recording the time required for reaching the 63% of steady state value of lateral force, then dividing it by the actual speed of tyre. Alternatively, λ is derived as the ratio between cornering stiffness C_{F_y} [N/rad] and lateral stiffness of tyre K_y [N/mm], as proposed in [9] (3).

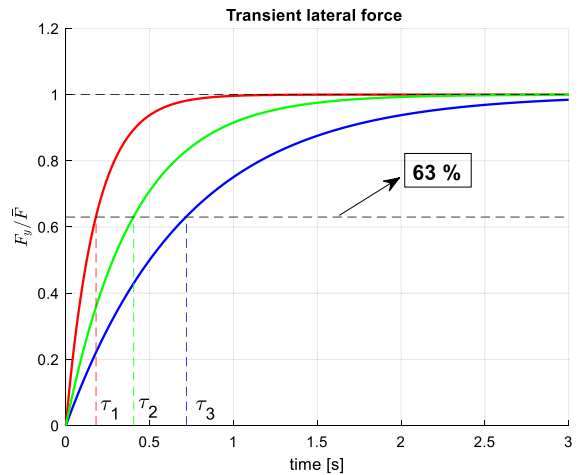


Fig. 1 Graphical solution of Eq. (1). The ratio $\frac{F_y}{\bar{F}}$ is depicted as function of time. Three lines represent three different tyres. When the ratio $\frac{F_y}{\bar{F}}$ reaches 63% of the steady state value, the relaxation length can be derived from abscissa axis

$$\lambda = \frac{C_{F_y}}{K_y} \tag{3}$$

In this paper the indirect evaluation of relaxation length is presented. Specifically, the role played by inflation pressure, vertical load and tyre wide on the relaxation length is investigated.

The direct method is complex to implement accurately, since it requires that the stiffness of test-rig is sufficient to sustain high loads without deforming. In addition, it is necessary to have an electric motor able to perform in milliseconds the step variation of slip angle. These aspects may cause a low signal-to-noise ratio, compromising the quality of the measurement. Considering this, it was chosen to evaluate the relaxation length through an easier but still accurate indirect method, as described in (3).

2 Methods and instruments

2.1 VeTyT test-rig

The evaluation of relaxation length through the indirect method requires the measurement of two parameters, specifically the tyre cornering stiffness and the lateral stiffness.

In this study, the measurement of the lateral force and lateral stiffness were performed through VeTyT, a testing machine specifically designed for measuring the mechanical characteristics of bicycle tyres [31]. It is the first test-rig for bicycle tyres in compliance with the standard ISO 9001-2015.

VeTyT consists of a rigid frame made from Aluminum 6060 T6, reinforced with plates and steel rods to ensure lightness and sufficient stiffness (Fig. 2). It is connected to the ground by means of Watt's linkage and universal joint. It has been conceived so that the longitudinal axis passes through the universal joint, the contact point tyre/surface and the centre of Watt's linkage. In this way, by rotating a shaft rigidly connected to the universal joint, the camber angle can be set. Furthermore, this solution allows compensating vertical vibrations of the wheel due to unevenness on the rolling surface. The tyre/road contact point can be displaced only in vertical direction, resulting in zero longitudinal slip.

The whole chassis can be tilted to set the camber angle in the range $\pm 25^\circ$, while the slip angle α can be adjusted by rotating the steering shaft. The vertical load acting on the wheel can be varied by adding masses on the frame. Its magnitude F_z is recorded

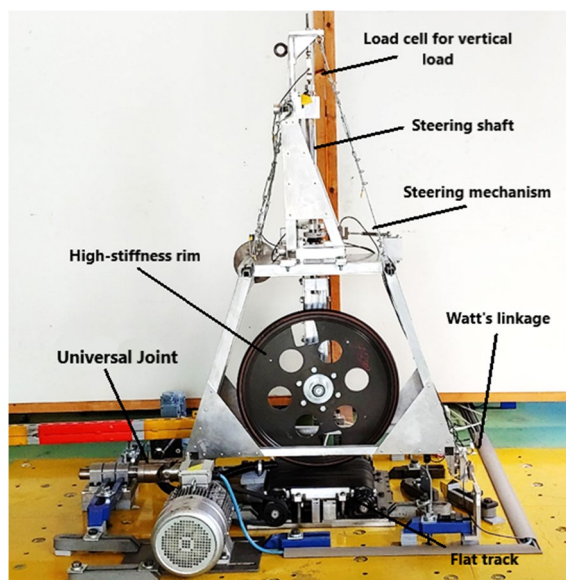


Fig. 2 VeTyT test-rig at Politecnico di Milano. The frame carries the bicycle tyre running on flat track. In this picture, tyre is mounted on high-stiffness laboratory rim [31]

by a load cell on the top of the steering shaft. The complete assembly of the test-rig is shown in Fig. 2.

As mentioned, the test-rig can be placed both on a drum, named “RuotaVia” [33], or on a flat track (Fig. 2). The drum has an outer diameter of 2.6 m, and it can reach a peripheral speed of 122 m/s. The flat track consists of a poly-V belt [36] moved by a 5 kW three-phase asynchronous electric motor. A maximum speed of 21 m/s can be achieved. An aluminum plate supports the flat track belt in the contact region. Pressured air mixed with silicone oil is blown between the plate and the flat track belt to reduce the friction.

In addition to standard commercial rims, the apparatus has been designed to accommodate special high-stiffness laboratory rim (the one mounted on in Fig. 2). In this way, the compliance of the rim does not affect the experimental measurements. Loads acting on tyre are presented in Fig. 3.

The cornering stiffness can be derived from post-processed data, as described in Sect. 2.2. Then, a proper set-up must be implemented for the static measurement of the lateral stiffness.

2.2 Fitting of experimental data

The experimental data collected during the tests were fitted by means of interpolating curves from Pacejka

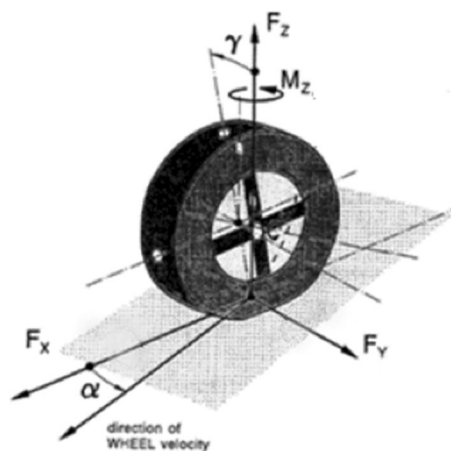


Fig. 3 Three-axis reference system used to derive forces, adapted from [35], with indicated the slip angle α and camber angle γ , the lateral force F_y , the longitudinal force F_x , the vertical force F_z and self aligning torque M_z .

Magic Formula [37, 38] as reported in (4). Data of lateral force F_y were firstly normalized with respect to the vertical load F_z .

$$\frac{F_y}{F_z} = D \sin\{C \arctan[B\alpha - E(B\alpha - \arctan(B\alpha))]\} + S_v \tag{4}$$

It is necessary to find the set of parameters which guarantee the best fitting between the experimental curves and the Pacejka’s formula. For this purpose, an iterative best-fitting method was exploited. The parameter S_v locates the center point of the curve with respect to the origin. D represents the peak value, B is the stiffness factor. C is the shape factor, while E has been introduced to determine the curvature at the peak [9]. The cornering stiffness (C_α , which corresponds to the slope at the origin of axis [9]) can be obtained by multiplying the parameters B , C and D as it follows (5)

$$C_\alpha = BCD \tag{5}$$

The cornering stiffness C_α allows to know the angular coefficient of the interpolating curve evaluated in $\alpha = 0^\circ$. Cornering stiffness is crucial to study the tyre response when subjected to different operative conditions such as inflation pressure or vertical load. Moreover, in [23, 39] the authors concluded the remarkable effect of tyre cornering stiffness C_α in the onset of dangerous dynamical instabilities.

The quality of the fitting method should be quantitatively assessed. Therefore, the correlation coefficient R^2 of the fitting of n experimental data was calculated in accordance with the following formula (6) [29, 40].

$$R^2 = 1 - \frac{\sum_i^n (y_i - f(x_i))^2}{\sum_i^n (y_i - \bar{y})^2} \tag{6}$$

The term \bar{y} is the mean value of the measured force, while $f(x_i)$ is the resulting value from the fitting formula (4). The correlation coefficient R^2 can vary between 0 and 1, according to the fitting quality. Higher values of R^2 mean a better fitting between the experimental data and the modeled ones.

2.3 Measurement of the lateral stiffness

The lateral stiffness per unit length K_y [N/mm] [1] is defined as the ratio between the lateral force F_y and

the lateral displacement of the carcass δ_{tyre} , according to (7)

$$K_y = \frac{F_y}{\delta_{tyre}} \tag{7}$$

VeTyT can be used also to measure the lateral displacement of the carcass (δ_{tyre}).

The tyre was mounted on high-stiffness laboratory rim while the slip and camber angles were set to zero. An aluminum plate covered with adhesive sandpaper was placed on the flat track, under the tyre to test.

The plate was pulled laterally, and its displacement was recorded by dial gauge (δ_p). Also, the displacement of the wheel rim was measured (δ_{rim}). Lateral displacement of the tyre only (δ_{tyre}) can be then evaluated as follows (8)

$$\delta_{tyre} = \delta_p - \delta_{rim} \tag{8}$$

The lateral force F_y responsible of the displacement δ_{tyre} was measured by VeTyT.

The whole set-up was arranged to reduce as much as possible the presence of undesired friction sources.

As for RuotaVia drum, a similar arrangement was implemented. Results were very similar but featured by a higher level of uncertainty since measuring the lateral stiffness on RuotaVia drum is a big challenge. Specifically, the results were affected by similar average values but large standard deviation. This forced us to rely only on lateral stiffness results measured on flat track. The current technological limitations of our set-up (designed primarily for flat track) make still do not allow us to obtain reliable lateral stiffness results on RuotaVia drum.

3 Measurements

The measurements were performed on three different premium tyres, mounted on high-stiffness laboratory rim with inner tube (Table 1). During the experimental campaign, different configurations of inflation pressure and vertical load were tested. First, the results of lateral stiffness measurement as well as a comparison between tyres are presented in Sect. 3.1. Then, the measurements of lateral force and the evaluation of cornering stiffness are discussed in Sect. 3.2.

Table 1 Tyres used for tests

	Width [mm]	ETRTO	Brand
Tyre1	26	700×26c	Brand #1
Tyre2	26	700×26c	Brand #2
Tyre3	28	700×28c	Brand #2

We tested tyres at three different vertical loads: 340 N, 400 N and 490 N. They are representative of common loads for a racing bicycle, considering the mass of common riders and bicycles. No standards for such bicycle tyre tests have been set so far.

Three different inflation pressures were tested, specifically 3.5 bar, 5.5 bar, and 7.5 bar. They were chosen to simulate an incorrect inflation pressure (or after punch), an intermediate pressure and the maximum recommended pressure. To have a benchmark for further analysis, a 26 mm wide tyre was tested both on flat track and RuotaVia drum [41]. The latter was used because cleat tests are made preferably on drums [42]. Therefore, it may be of interest also to test on drum and set benchmarks for further analysis, even if we know that the drum curvature affects the tyre contact patch shape.

3.1 Lateral stiffness

The lateral stiffness was measured according to the set-up presented in Sect. 2.3.

The measured lateral force F_y applied to the tyre is plotted as function of the lateral displacement δ_{tyre} in Fig. 4, for vertical load equal to 340 N (results for Tyre1 are shown).

The relationship shown in Fig. 4 is linear for all the tested inflation pressures. As expected, large force is required to obtain the same displacement if the tyre is inflated more.

Since the relationship between lateral force and displacement is linear, the lateral stiffness can be directly derived as the slope of the curves evaluated in the origin of axis. Similar behavior was found for the other tested tyres.

The tests were repeated for vertical loads equal to 400 N and 490 N. The results of lateral stiffness as function of vertical load for Tyre1 and Tyre2 are plotted in Fig. 5, for different inflation pressures.

The results in Fig. 5 prove that the lateral stiffness K_y largely depends on inflation pressure. As

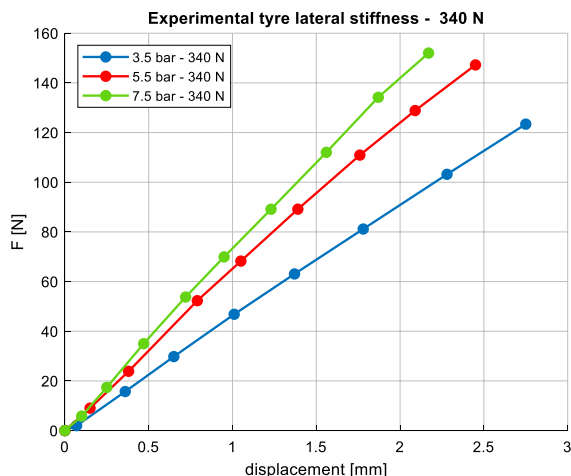
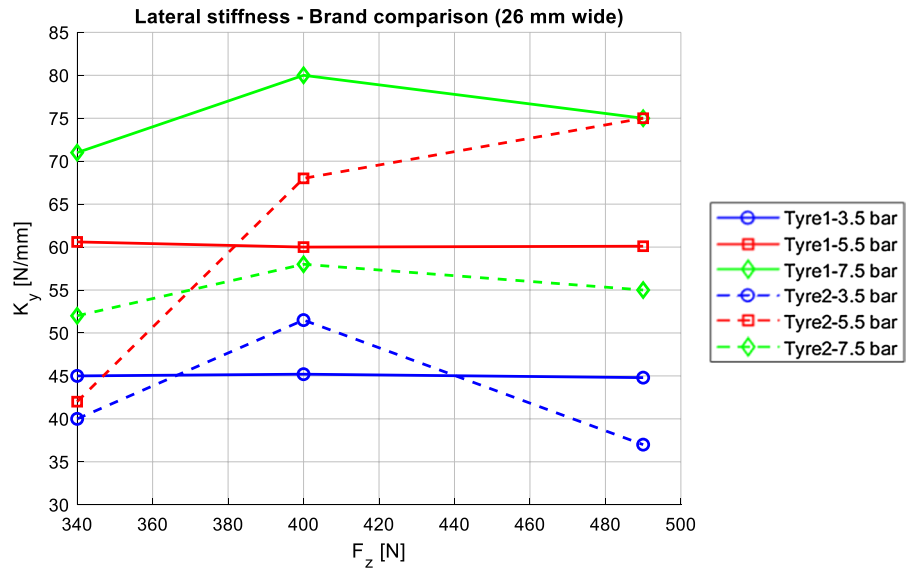


Fig. 4 Applied lateral force as function of displacement, recorded through dial gauges. The results for Tyre1 (26 mm wide tyre) are shown

for Tyre1, the variation of vertical load does not appear to have a great influence on lateral stiffness, especially for low pressures (3.5 bar and 5.5 bar, the blue and red line respectively). A limited influence of vertical load on lateral stiffness seems to occur only for pressure equal to 7.5 bar, where a variation in the order of 10% is recorded changing the vertical load. On the contrary, Tyre2 is affected by the variation in vertical load as well as pressure variations. Lateral stiffness for low inflation pressure (3.5 bar) is almost the same for the tested tyres; nonetheless, Tyre2 (blue dashed line) seems to increase up to 20% when the vertical load passes from 340 to 400 N. A large difference was found between Tyre1 and Tyre2 inflated at 5.5 bar. While the lateral stiffness for Tyre1 at 5.5 bar is basically independent of vertical load, Tyre2 is affected a lot by variation in F_z . At 5.5 bar, it shows an increasing trend with the vertical load, reaching higher values than the ones measured for the same tyre at 7.5 bar. On the contrary for what observed at 5.5 bar, the lateral stiffness for Tyre2 resulted to be 25% lower than the outcome for Tyre1 for inflation pressure equal to 7.5 bar. This may be explained by the different tyre manufacturing process. While Tyre1 is obtained from a single compound, Tyre2 is featured by the superimposition of different compounds layers added with graphene and silice, glued and pressed together. This may result in a

Fig. 5 Lateral stiffness as function of vertical load. Three different inflation pressures were tested, for three vertical loads. Results from tyres of different brands but equal wide (26 mm) are depicted



tyre more sensitive to pressure variation, narrowing the optimal inflation pressure range.

These features may be of strong practical and computational interest since they are related to realistic scenarios. It could be a feasible riding case when the cyclist approaches a downhill or it moves forward the chest for sprinting (referring to a front wheel). It means that tyres may show different behavior in different circumstances.

A comparison between tyres of the same brand but different wide was then carried out, for different inflation pressures and vertical loads (Fig. 6).

Tyre2 (26 mm wide) showed larger lateral stiffness if compared to Tyre3 (28 mm wide), for the same inflation pressure. Similarly to what already pointed out for Tyre2 in Fig. 5, the lateral stiffness for Tyre3 at 5.5 bar resulted to be higher than the one measured at 7.5 bar, for the same tyre at vertical loads larger than 400 N. It is worth noticing that Tyre2 and Tyre3 are featured by the same manufacturing process, so that the results in Fig. 6 are confirming the outcomes discussed in Fig. 5.

3.2 Cornering stiffness

VeTyT was used to measure the lateral force of the tested tyre, varying slip angle, inflation pressure and vertical load. The cornering stiffness C_{F_y} was then derived from the model described in Sect. 2.2, according to (2.2). The tests were performed on flat track

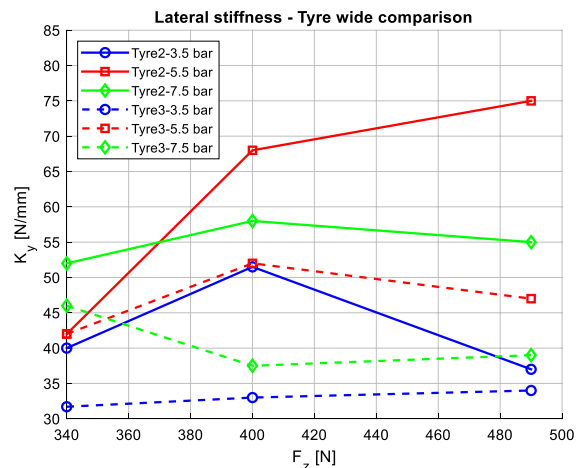


Fig. 6 Lateral stiffness as function of vertical load. Three different inflation pressures were tested, for three vertical loads. Results of different wide tyres are depicted (Tyre2: 26 mm wide; Tyre3: 28 mm wide)

and on RuotaVia drum for Tyre1, on flat track only for Tyre 2 and Tyre3. The rolling speed of the test was set at 9.3 km/h, as a result of an iterative process to reduce as much as possible the detrimental increase in temperature of the rolling surface [43].

To study the combined effect of inflation pressure and vertical load variation, data are plotted in form of carpet plot. It is possible to observe the curves of lateral force exerted by the tyre as function of different vertical loads, inflation pressures and slip

angles. The analysis was carried out on slip angles α up to 4° , since the aim of this work is to evaluate of the cornering stiffness.

The results in Fig. 7 come from tests on flat track, for tyre mounted on high-stiffness laboratory rim. The curves for inflation pressure equal to 3.5 bar (yellow curves in Fig. 7) result in a lower cornering stiffness, for each vertical load tested. The same behavior cannot be observed for tests on RuotaVia drum (Fig. 8), where for vertical load equal to 340 N the trend is completely inverted with respect to that shown in Fig. 7. The reason of this phenomenon may be related to the different contact patch geometry. The contact patch area is smaller for RuotaVia drum [41], due to the geometrical characteristics of the contact surface.

The cornering stiffnesses of the analyzed cases in Figs. 7 and 8 were then evaluated, according to (2.2). The results are shown in Fig. 9 both for flat track and RuotaVia tests.

Cornering stiffness measured on flat track is on average 15% higher than the one measured on RuotaVia, since it may be affected by different shape of contact patch [41].

Referring to flat track, cornering stiffness C_{F_y} increases with vertical load, for pressures equal to 5.5 bar and 7.5 bar. Considering inflation pressure of 3.5 bar, C_{F_y} slightly decreases for vertical loads

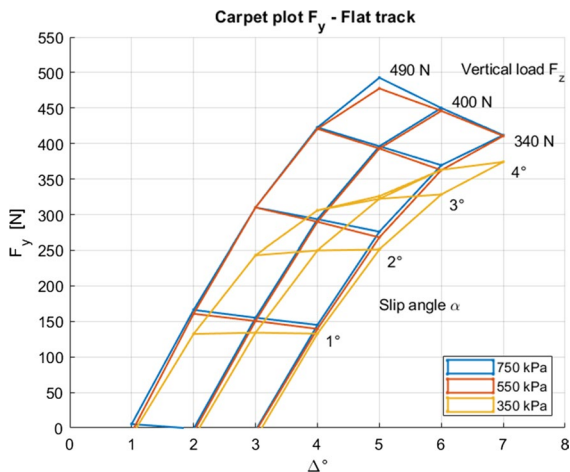


Fig. 7 Carpet plot showing the lateral force for a combination of inflation pressures and vertical loads. Tests were performed with tyre mounted on high-stiffness rim, on flat track. Tyre1 (26 mm width) was tested

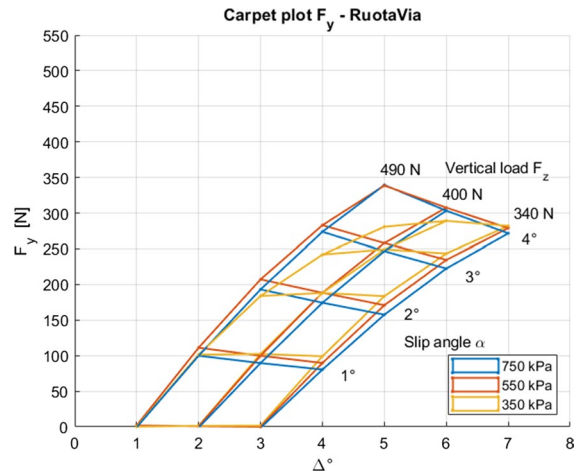


Fig. 8 Carpet plot showing the lateral force for a combination of inflation pressures and vertical loads. Tests were performed with tyre mounted on high-stiffness rim, on RuotaVia drum. Tyre1 (26 mm width) was tested

higher than 400 N. For pressure equal to 7.5 bar and vertical load 340 N it is smaller than for other inflation pressures.

The peak value of cornering stiffness for high vertical load (490 N) was found for larger inflation pressure, i.e., 7.5 bar. It is worth noticing that this behavior corresponds to the expected one, since higher pressures are needed to ensure better performances for higher vertical loads. On the contrary, reduced inflation pressures are advised for smaller vertical loads.

As for tests on RuotaVia drum, they show a different trend of cornering stiffness with respect to the flat track. The cornering stiffness appears to increase with the vertical load. At lower values of vertical load, C_{F_y} is higher for low inflation pressures. For F_z equal to 340 N, the cornering stiffness at 3.5 bar is 15% higher than at 7.5 bar. The peak of cornering stiffness at 490 N was found for inflation pressure of 5.5 bar.

The influence of vertical load on cornering stiffness is smaller on flat track than on RuotaVia [41]. The trend of C_{F_y} on RuotaVia and the difference in magnitude with respect to the flat track may be due to the smaller contact patch area, as mentioned before.

The cornering stiffnesses depicted in Fig. 9 are summarized in Tables 2 and 3 for flat track and RuotaVia, respectively.

Fig. 9 Cornering stiffness for different inflation pressures, as function of vertical load. Comparison between tests on flat track (FT) and on RuotaVia drum (RV) (Tyre1, 26 mm wide)

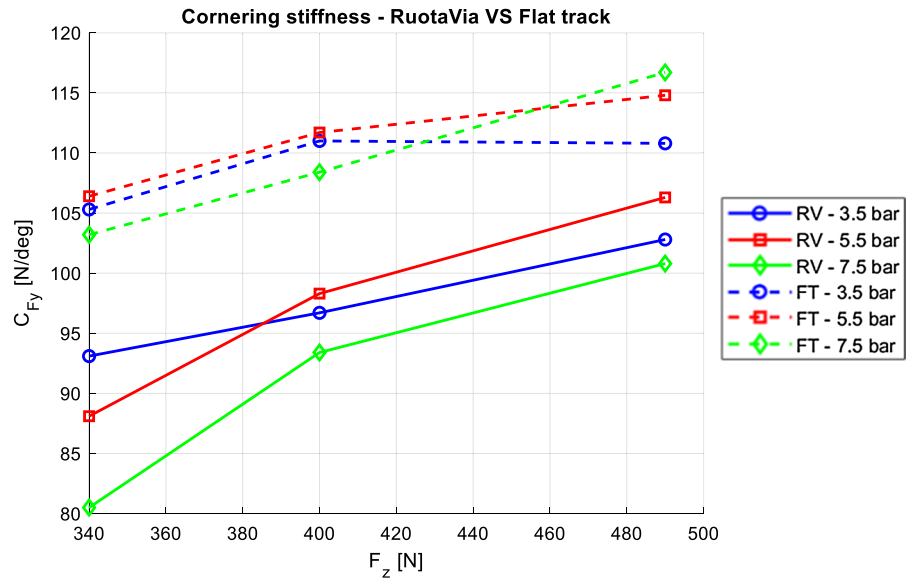


Table 2 Cornering stiffness values at different inflation pressures and vertical loads, for tests on flat track. A 26 mm wide tyre was tested (Tyre1)

C_{F_y} [N/deg]	p[bar]		
Tyre1—Flat track	3.5	5.5	7.5
F_z [N]			
340	105.3	106.4	103.2
400	111.1	111.7	108.4
490	110.7	114.8	116.7

Table 3 Cornering stiffness values at different inflation pressures and vertical loads, for tests on RuotaVia drum. A 26 mm wide tyre was tested (Tyre1)

C_{F_y} [N/deg]	p[bar]		
Tyre1—RuotaVia	3.5	5.5	7.5
F_z [N]			
340	93.1	88.1	80.5
400	96.7	98.3	93.4
490	102.8	106.3	100.8

The comparison between same wide tyres (26 mm) but different brands was then carried out. As aforementioned, they are featured by different manufacturing processes, layers and compounds.

The tyres were tested on flat track, mounted on high stiffness rim with the same inner tube. The measured cornering stiffness is depicted in Fig. 10.

The cornering stiffnesses of Tyre1 are higher than those of Tyre2 for each value of inflation pressure and vertical load. The peak value for vertical load 490 N is obtained for pressure equal to 7.5 bar for Tyre1, while for pressure 3.5 bar for Tyre2.

The cornering stiffness for Tyre2 follows an increasing trend with vertical load, for each value of internal pressure. For F_z equal to 490 N, C_{F_y} for Tyre2 is equal to the corresponding one for Tyre1. The latter has already reached its saturation limit since it shows a decrease in C_{F_y} . Contrarily, Tyre2 seems to sustain higher vertical load before reaching the saturation limit.

The results of cornering stiffness for Tyre1 (measured on flat track) and Tyre2 are reported in Tables 2 and 4, respectively.

Observing Fig. 11, larger tyre (Tyre3) is able to generate higher cornering stiffness for each value of inflation pressure and vertical load. Results for Tyres 2 and 3 depicted in Fig. 11 follow an increasing trend, without reaching the saturation limit even for the largest vertical load (490 N). The mean difference between cornering stiffness for Tyre2 and Tyre3 is on average 8 N/deg (~6%).

The results of cornering stiffness for Tyre2 and Tyre3 are reported in Tables 4 and 5, respectively.

Fig. 10 Cornering stiffness for different inflation pressures, as function of vertical load. Comparison between tests with Tyre1 and Tyre2 (26 mm wide, different brand)

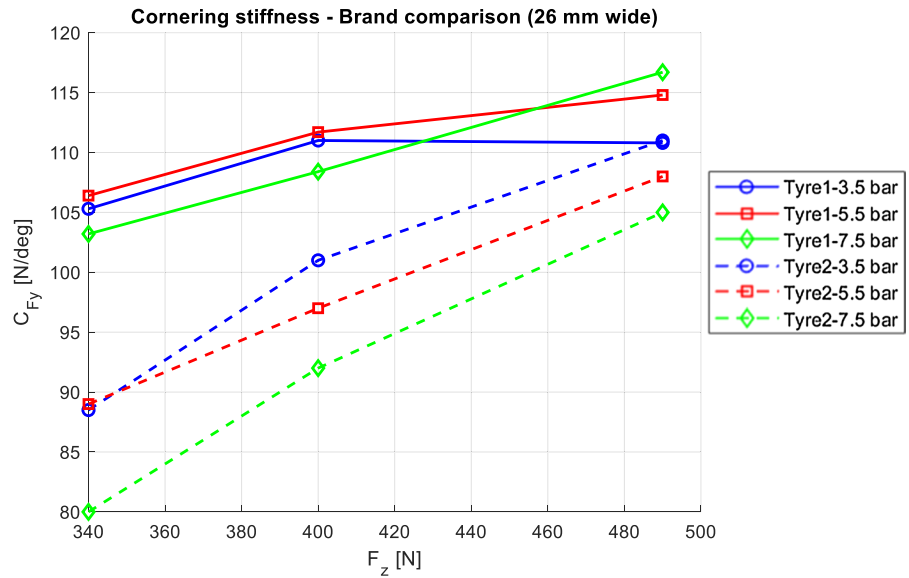


Table 4 Cornering stiffness values at different inflation pressures and vertical loads. A 26 mm wide tyre was tested on flat track (Tyre2)

C _{Fy} [N/deg]	p[bar]		
Tyre2—Flat track	3.5	5.5	7.5
F _z [N]			
340	88.5	88.8	80.1
400	101.0	97.2	92.0
490	110.7	107.9	105.0

4 Evaluation of Relaxation length

The relaxation length can be computed according to (1.3). Firstly, a comparison between results on flat track and RuotaVia drum is presented.

According to Fig. 12, relaxation length tends to increase with the increase of vertical load. Moreover, it also increases while pressure decreases, meaning that the tyre becomes less responsive for low pressure values. Data of each measurement are summarized in

Fig. 11 Cornering stiffness for different inflation pressures, as function of vertical load. Comparison between Tyre2 (26 mm wide) and Tyre3 (28 mm wide)

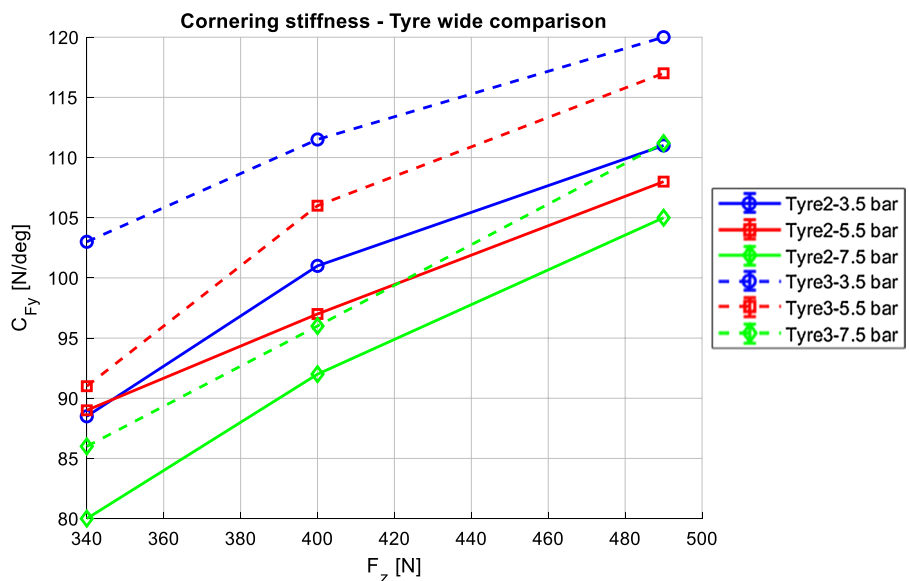


Table 5 Cornering stiffness values at different inflation pressures and vertical loads. A 28 mm wide tyre was tested on flat track (Tyre3)

C_{F_y} [N/deg]	p[bar]		
	3.5	5.5	7.5
Tyre3—Flat track			
F_z [N]			
340	103.6	91.0	86.2
400	111.5	105.8	95.6
490	120.0	117.2	111.2

Tables 6 and 7. An uncertainty of 3 mm was introduced for relaxation length values, according to the analysis presented in [31].

We found that the relaxation length is generally lower for RuotaVia drum, due to the smaller value of cornering stiffness, as stated before in Sect. 3.2.

It was discovered the large variation in relaxation length due to inflation pressure. Relaxation length is almost doubled when passing from inflation pressure of 3.5 bar to 7.5 bar, both for RuotaVia and flat track for the same vertical load. This proves the large role played by inflation pressure on the relaxation length, therefore on the responsiveness of the tyre.

Relaxation length for same wide tyres (26 mm) but from different brands were then analyzed. For a direct comparison, the results are plotted in Fig. 13.

Table 6 Relaxation length values, for a combination of inflation pressures and vertical loads. This is referred to the measurements on flat track, for 26 mm wide tyre (Tyre1)

$\lambda_{\text{Flattrack}}$ [mm]	p[bar]		
	3.5	5.5	7.5
Tyre1			
F_z [N]			
340	134.0	100.9	78.6
400	141.5	106.0	82.6
490	140.9	108.9	88.9

Observing Fig. 13, the relaxation length of Tyre2 appears more sensitive to variation in vertical load than for Tyre1.

Considering inflation pressure of 7.5 bar, the trend of Tyre1 and Tyre2 is very similar but shifted on average by 13%. Tyre2 at pressure of 3.5 bar reaches the peak of relaxation length for vertical load 490 N, with a difference of +24% with respect to Tyre1.

The lowest relaxation length can be found for Tyre2 at vertical load 490 N and inflation pressure of 5.5 bar (Tables 8, 9).

According to the results presented in Fig. 14, a 28 mm wide tyre (Tyre3) has higher relaxation length if compared to 26 mm wide one (Tyre2). We can conclude that 28 mm wide racing tyre is less responsive in turning maneuvers with respect to the tighter one.

Fig. 12 Relaxation length evaluated for different pressure values and vertical loads, for Tyre1 (26 mm wide). Dashed lines represent the measurements on Flat track (FT), while continuous lines are for tests on RuotaVia (RV)

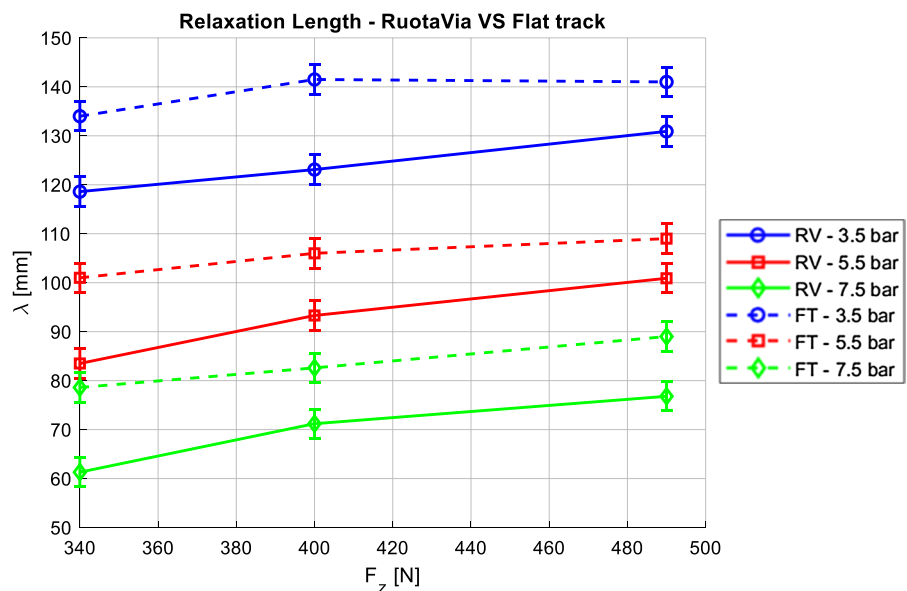


Table 7 Relaxation length values, for a combination of inflation pressures and vertical loads. This is referred to measurements on flat track. Tyre1 (26 mm wide) was tested

$\lambda_{\text{RuotaVia}}[\text{mm}]$ Tyre1	p[bar]		
	3.5	5.5	7.5
$F_z[\text{N}]$			
340	118.6	83.5	61.3
400	123.1	93.3	71.2
490	130.9	100.9	76.8

Nonetheless, 28 mm wide tyre (Tyre3) can carry higher vertical and lateral loads (Fig. 11).

The relaxation length of both Tyre2 and Tyre3 is higher for pressure 7.5 bar than for pressure 5.5 bar. As already observed for lateral stiffness in Fig. 6, this may be due to the manufacturing process featured by the superimposition of different compound layers. We hypothesize that at high pressure a kind of micro slippage between the layers may appear, leading to a decrease in relaxation length.

A comparison of the results presented in this paper with the ones obtained by other researchers cannot be carried out since there is a lack of information on how the tests were performed. Moreover, they tested different kind of tyres, not for racing bicycles so that a direct comparison may be useless and meaningless.

In [30], the relaxation length was evaluated on flat track for different bicycle tyres, applying a vertical load of 430 N and inflating at the suggested pressure (not declared). The values were in the range of 40–60 mm, less than those obtained in this paper. The authors highlighted some flexibility in the frame which carried the tyres that might have affected the measurements.

In [18], tests were performed on scooter tyres, for different inflation pressures and tyre sizes. Values in the range 54–96 mm were found for relaxation length, much closer to those presented in this paper. Again, this is not a reasonable comparison, as scooter tyres are designed for greater loads.

5 Conclusions

The paper presents the results of the relaxation length related to the lateral force for road racing bicycle

Table 8 Relaxation length values, for a combination of inflation pressures and vertical loads. This is referred to measurements on flat track. A 26 mm wide tyre was tested (Tyre2)

$\lambda_{\text{Tyre2}}[\text{mm}]$	p[bar]		
	3.5	5.5	7.5
$F_z[\text{N}]$			
340	126.7	121.1	88.3
400	112.0	81.7	90.5
490	175.8	82.1	108.9

Table 9 Relaxation length values, for a combination of inflation pressures and vertical loads. This is referred to measurements on flat track. Tyre3 (28 mm wide) was tested

$\lambda_{\text{Tyre3}}[\text{mm}]$	p[bar]		
	3.5	5.5	7.5
$F_z[\text{N}]$			
340	187.3	123.2	107.4
400	192.2	115.5	145.8
490	198.5	143.3	163.3

tyres. It has been derived as the ratio between cornering stiffness C_{F_y} [N/rad] and lateral stiffness K_y of the tyre.

A 26 mm wide tyre was tested both on flat track and drum of 2.6 m of diameter (named “RuotaVia drum”). The curvature of the drum may affect the length and the shape of contact tyre/ground. Considering this, the cornering stiffness on flat track resulted in 15% higher values. Consequently, relaxation length on flat track is on average 11% larger than the outcomes from RuotaVia drum, for inflation pressure of 7.5 bar.

A comparison was then performed on same wide tyres (26 mm) but different brands, tested on flat track. Differences were found both on lateral stiffness and cornering stiffness. The relaxation length was very sensitive to the variation in inflation pressure. It almost doubled when passing from inflation pressure of 3.5 bar to 7.5 bar, for the same vertical load. Conversely, the tyre of the second brand was affected both by inflation pressure and vertical load (same wide tyres).

A 28 mm wide tyre was then tested, so as to compare the outcomes with the corresponding 26 mm wide one (same brand). Both the cornering stiffness

Fig. 13 Relaxation length evaluated for different pressure values and vertical loads, for Tyre1 and Tyre2 (26 mm wide). Tests performed on flat track

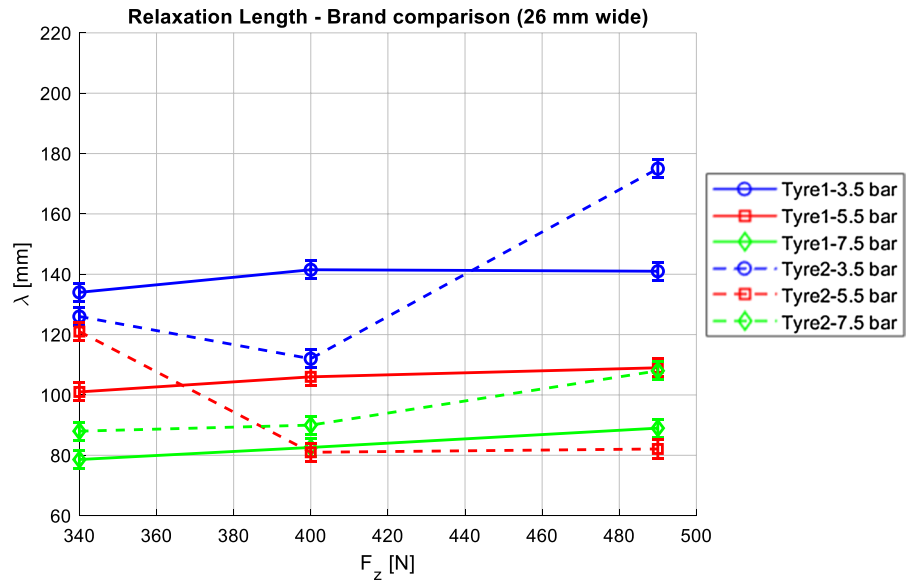
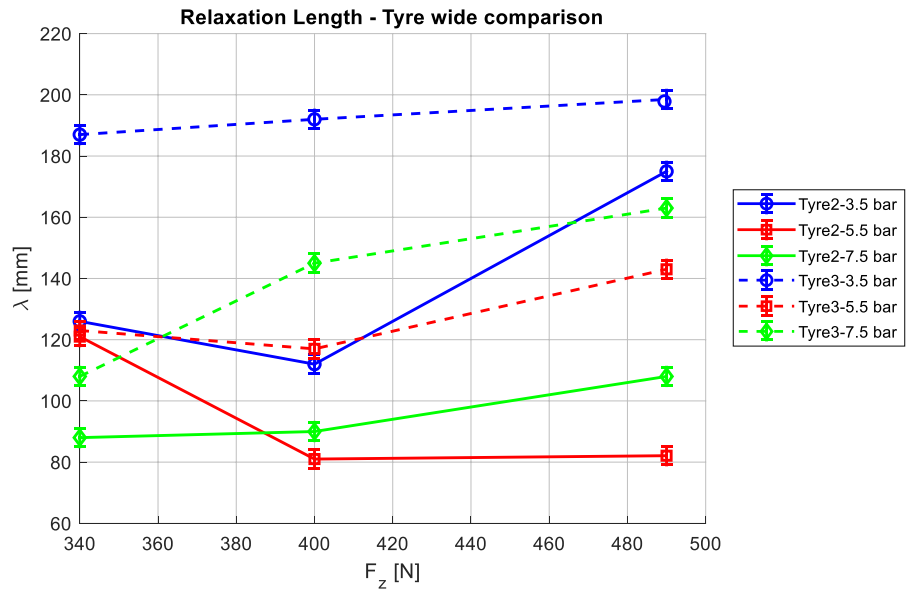


Fig. 14 Relaxation length evaluated for different pressure values and vertical loads, for Tyre2 and Tyre3 (respectively, 26 mm and 28 mm wide tyres of the same brand). Results derive from tests on flat track



and relaxation length of 28 mm wide tyre was higher than the 26 mm wide one.

Summarizing the analyses presented in the paper, the following conclusions may be drawn.

- There are no protocols to evaluate relaxation length for bicycle tyres. Moreover, no studies on racing bicycle tyres seem to exist. This paper provides a preliminary result to try to close the gap.
- Some attempts to measure bicycle tyre characteristics have been made, nonetheless a reliable evaluation of relaxation length is hard to find. We try to foster the development of a database of bicycle tyre parameters through accurate measurements.
- The relaxation length increases with the vertical load. In addition, we noted that the relaxation length is much more sensitive to variation of inflation pressure than of vertical load for a tyre of a specific brand. Conversely, the tyre of second

brand was affected both by inflation pressure and vertical load.

- The differences revealed between the same wide tyres but different brands may be due to some peculiarities in manufacturing process.

A 28 mm wide tyre is less responsive than 26 mm wide one, of the same brand, since it showed higher values of relaxation length. Nonetheless, it is able to carry higher vertical loads, and the cornering stiffness resulted on average 6% higher than for 26 mm wide tyre. In the future, the evaluation of relaxation length will be performed for different type of tyres (trekking bicycle tyres, cargo-bike tyres, etc.), with the method derived in this paper. These data may help the advancement in the field of bicycle dynamics, with the aim of improving safety and performances.

Acknowledgements The authors thank Isabel Pollini, Vincenzo Tartaglione and Prof. Giorgio Previati for their support during the months of experimental test campaign. Many thanks to Mario Pennati, always willing to help us.

Funding Open access funding provided by Politecnico di Milano within the CRUI-CARE Agreement.

Declarations

Conflict of interest The authors report there are no competing interests to declare.

Open Access This article is licensed under a Creative Commons Attribution 4.0 International License, which permits use, sharing, adaptation, distribution and reproduction in any medium or format, as long as you give appropriate credit to the original author(s) and the source, provide a link to the Creative Commons licence, and indicate if changes were made. The images or other third party material in this article are included in the article's Creative Commons licence, unless indicated otherwise in a credit line to the material. If material is not included in the article's Creative Commons licence and your intended use is not permitted by statutory regulation or exceeds the permitted use, you will need to obtain permission directly from the copyright holder. To view a copy of this licence, visit <http://creativecommons.org/licenses/by/4.0/>.

References

- Loeb JS, Guenther DA, Chen HHH, Ellis JR (1990) Lateral stiffness, cornering stiffness and relaxation length of the pneumatic tire. *SAE Tech Papers* 99:147–155. <https://doi.org/10.4271/900129>
- Schwab AL, Meijaard JP (2013) A review on bicycle dynamics and rider control. *Veh Syst Dyn* 51(7):1059–1090. <https://doi.org/10.1080/00423114.2013.793365>
- Meijaard JP, Papadopoulos JM, Ruina A, Schwab AL (2007) Linearized dynamics equations for the balance and steer of a bicycle: a benchmark and review. *Proc R Soc A: Math Phys Eng Sci* 463(2084):1955–1982. <https://doi.org/10.1098/rspa.2007.1857>
- Romano L, Bruzelius F, Jacobson B (2020) Brush tyre models for large camber angles and steering speeds. *Veh Syst Dyn*. <https://doi.org/10.1080/00423114.2020.1854320>
- Cossalter V, Lot R, Maggio F (2004) The modal analysis of a motorcycle in straight running and on a curve. *Meccanica* 39(1):1–16. <https://doi.org/10.1023/A:1026269926222>
- Guo K, Lu D, Wu H (2018) Tire dynamics collaborative development strategy. *Chin J Eng Sci* 20(1):91. <https://doi.org/10.15302/j-sscae-2018.01.013>
- Lu D, Lu L, Wu H, Wang W, Lv M (2020) Tire dynamics modeling method based on rapid test method. *Chin J Mech Eng*. <https://doi.org/10.1186/s10033-020-00513-8>
- Cossalter V, Doria A, Giolo E, Taraborrelli L, Massaro M (2014) Identification of the characteristics of motorcycle and scooter tyres in the presence of large variations in inflation pressure. *Veh Syst Dyn* 52(10):1333–1354. <https://doi.org/10.1080/00423114.2014.940981>
- Pacejka H (2005) *Tire and vehicle dynamics*. Elsevier, New York. <https://doi.org/10.1016/B978-0-7506-6918-4.X5000-X>
- Moore JK, Hubbard M, Schwab AL, Kooijman JDG (2010) Accurate measurement of bicycle parameters. *Bicycle and motorcycle dynamics: symposium on the dynamics and control of single track vehicles*, pp 20–22
- Sharp RS (2008) On the stability and control of the bicycle. *Appl Mech Rev* 61(1–6):0608031–06080324. <https://doi.org/10.1115/1.2983014>
- Cossalter V (2006) *Motorcycle dynamics*
- Bulsink VE, Doria A, Van De Belt D, Koopman B (2015) The effect of tyre and rider properties on the stability of a bicycle. *Adv Mech Eng*. <https://doi.org/10.1177/1687814015622596>
- Sharp RS (1971) The stability and control of motorcycles. *J Mech Eng Sci* 13(5):316–329
- Uil RT, Schmeitz AJC, Besselink IJM, Nijmeijer H (2006) Non-lagging effect of motorcycle tyres—an experimental study with the Flat Plank Tyre Tester. In: Eindhoven University of Technology, Department of Mechanical Engineering
- Bucchi F, Cerù F, Frenzo F (2017) Stability analysis of a novel four-wheeled motorcycle in straight running. *Meccanica* 52(11–12):2603–2613. <https://doi.org/10.1007/s11012-017-0645-x>
- Cossalter V, Lot R, Massaro M (2011) An advanced multibody code for handling and stability analysis of motorcycles. *Meccanica* 46(5):943–958. <https://doi.org/10.1007/s11012-010-9351-7>
- Doria A, Taraborrelli L (2016) Out-of-plane vibrations and relaxation length of the tyres for single-track vehicles. *Proc Inst Mech Eng Part D: J Automobile Eng* 230(5):609–622. <https://doi.org/10.1177/0954407015590703>

19. Besselink IJM, Schmeitz AJC, Pacejka HB (2010) An improved Magic Formula/Swift tyre model that can handle inflation pressure changes. *Veh Syst Dyn* 48(Suppl1):337–352. <https://doi.org/10.1080/00423111003748088>
20. Dell’Orto G, Ballo FM, Mastinu G (2022) Experimental methods to measure the lateral characteristics of bicycle tyres—a review. *Veh Syst Dyn*. <https://doi.org/10.1080/00423114.2022.2144388>
21. Cossalter V, Doria A, Lot R, Ruffo N, Salvador M (2003) Dynamic properties of motorcycle and scooter tires: measurement and comparison. *Veh Syst Dyn* 39(5):329–352. <https://doi.org/10.1076/vesd.39.5.329.14145>
22. Previati G, Magnani G, Mastinu G (2019) Analysis of bicycle shimmy and relevant bicycle compliances. In: Proceedings, bicycle and motorcycle dynamics 2019 symposium on the dynamics and control of single track vehicles, 2019, Accessed: Jan. 05, 2023. Available: https://bmd2019.figshare.com/articles/conference_contribution/Analysis_of_Bicycle_Shimmy_and_Relevant_Bicycle_Compliances/12363707
23. Tomiati N, Magnani G, Scaglioni B, Ferretti G (2017) Model Based analysis of shimmy in a racing bicycle. In: Proceedings of the 12th International modelica conference, Prague, Czech Republic, May 15–17, 2017, Linköping University Electronic Press, pp 441–447. doi: <https://doi.org/10.3384/ecp17132441>.
24. Klinger F, Nusime J, Edelmann J, Plöchl M (2014) Wobble of a racing bicycle with a rider hands on and hands off the handlebar. *Veh Syst Dyn* 52:51–68. <https://doi.org/10.1080/00423114.2013.877592>
25. Doria A, Roa Melo SD (2018) On the influence of tyre and structural properties on the stability of bicycles. *Veh Syst Dyn* 56(6):947–966. <https://doi.org/10.1080/00423114.2017.1403032>
26. Plöchl M, Edelmann J, Angrosch B, Ott C (2012) On the wobble mode of a bicycle. *Veh Syst Dyn* 50(3):415–429. <https://doi.org/10.1080/00423114.2011.594164>
27. Souh B (2015) Influence of tire side forces on bicycle self-stability. *J Mech Sci Technol* 29(8):3131–3140. <https://doi.org/10.1007/s12206-015-0711-z>
28. Roa S, Doria A, Muñoz L (2018) Optimization of the bicycle weave and wobble modes. In: ASME 2018 International design engineering technical conferences and computers and information in engineering conference IDETC, Quebec City, Canada. doi: <https://doi.org/10.1115/DETC2018-86132>
29. Doria A, Tognazzo M, Cusimano G, Bulsink V, Cooke A, Koopman B (2013) Identification of the mechanical properties of bicycle tyres for modelling of bicycle dynamics. *Veh Syst Dyn* 51(3):405–420. <https://doi.org/10.1080/00423114.2012.754048>
30. Dressel A, Rahman A (2012) Measuring sideslip and camber characteristics of bicycle tyres. *Veh Syst Dyn* 50:1365–1378. <https://doi.org/10.1080/00423114.2011.615408>
31. Dell’Orto G, Ballo FM, Mastinu G, Gobbi M (2022) Bicycle tyres—development of a new test-rig to measure mechanical characteristics. *Measurement* 202:111813. <https://doi.org/10.1016/j.measurement.2022.111813>
32. Uslenghi L, Vaccari L (2021) Indoor testing of cycling tyres and quality assurance of ‘Vetyt’ test rig. MSc. Thesis, Politecnico di Milano
33. Gobbi M, Mastinu G, Pennati M (2008) Indoor testing of road vehicle suspensions. *Meccanica* 43(2):173–184. <https://doi.org/10.1007/s11012-008-9119-5>
34. Mitschke M, Wallentowitz H (2014) *Dynamik der Kraftfahrzeuge*. Springer Fachmedien Wiesbaden, Weisbaden. <https://doi.org/10.1007/978-3-658-05068-9>
35. Unrau H, Zamow J (1997) TYDEX-Format Manual Release 1.3. Description and Reference Manual, pp 1–55
36. SpA PTM Poly-V belts and pulleys
37. Bakker E, Pacejka HB, Lidner L (1989) A new tire model with an application in vehicle dynamics studies. *SAE Technical Papers* 98:101–113. <https://doi.org/10.4271/890087>
38. Bakker E, Nyborg L, Pacejka HB (1987) Tyre modelling for use in vehicle dynamics studies. *SAE Tech Papers*. <https://doi.org/10.4271/870421>
39. Tomiati N, Colombo A, Magnani G (2019) A nonlinear model of bicycle shimmy. *Veh Syst Dyn* 57(3):315–335. <https://doi.org/10.1080/00423114.2018.1465574>
40. Asuero AG, Sayago A, González AG (2006) The correlation coefficient: an overview. *Crit Rev Anal Chem* 36(1):41–59. <https://doi.org/10.1080/10408340500526766>
41. Mastinu G, Pennati M, Gobbi M (2002) Design and construction of a test rig for assessing tyre characteristics at rollover. *SAE Tech Papers*. <https://doi.org/10.4271/2002-01-2077>
42. Gobbi M, Giorgetta F, Guarneri P, Rocca G, Mastinu G (2006) Experimental study and numerical modeling of the dynamic behaviour of tyre/suspension while running over an obstacle. *ASME Int Mech Eng Congress Expos* 2006:195–204
43. Dell’Orto G, Mastinu G (2022) Effect of temperature on the mechanical characteristics of bicycle tyres. In: International cycling safety conference 2022, Dresden

Publisher’s Note Springer Nature remains neutral with regard to jurisdictional claims in published maps and institutional affiliations.